RELATIONSHIPS BETWEEN MICROSTRUCTURE AND MECHANICAL PROPERTIES OF CELLULAR CORNSTARCH EXTRUDATES

RODERICK AGBISIT[1], SAJID ALAVI[1,3], ENZHI CHENG[1], THOMAS HERALD[2] and ALLEN TRATER[1]*

[1]*Department of Grain Science and Industry*

[2]*Institute of Food Science*
Kansas State University
Manhattan KS 66506

Received for Publication March 3, 2006
Accepted for Publication January 12, 2007

ABSTRACT

Relationships between mechanical properties and microstructure of brittle biopolymer foams were investigated using noninvasive imaging as a tool. Cornstarch was processed in a twin-screw extruder to produce brittle foams with varying microstructure. X-ray microtomography was used to measure microstructure features of the foams, including average cell diameter (2.07–6.32 mm), cell wall thickness (0.13–0.25 mm) and cell number density (18–146 cm^{-3}). Mechanical properties, including compression modulus (2.2–7.8 MPa), crushing stress (42–240 kPa), number of spatial ruptures (2.6–3.6 mm^{-1}), average crushing force (22–67 N) and crispness work (6.4–22 N·mm), were determined instrumentally. Compression modulus had a reasonably good fit ($R^2 = 0.72$) with the Gibson–Ashby model for brittle foams, while crushing stress did not fit as well ($R^2 = 0.41$). Cellular characteristics had moderate to high correlation ($|r| = 0.48–0.81$) with mechanical properties, and provided significant insight into the deformation mechanism of the foams.

PRACTICAL APPLICATIONS

Mechanical properties of extruded biopolymeric foams are largely determined by their microstructure, but the relationships involved have not been properly understood. This study used mechanical testing in combination with

[3] Corresponding author. TEL: 785-532-2403; FAX: 785-532-4017; EMAIL: salavi@ksu.edu
* Present address: Frito Lay R&D, 7701 Legacy Drive, Plano, TX 75024

noninvasive x-ray microtomography to investigate these relationships. Results from this study furthered understanding of the deformation mechanism of brittle foams, and represent an important step toward the ability to better design crisp and crunchy food products with desired textures.

KEYWORDS

Extrusion, foams, microstructure mechanical properties, noninvasive imaging, x-ray microtomography

INTRODUCTION

In an effort to understand the physical and rheological behavior as well as the mechanical and sensory attributes of foods, processing focus and emphasis have shifted to the microstructure level (less than 100 μm). Microstructure elements such as air bubbles or cells, starch granules, protein assemblies and food biopolymer matrices contribute greatly to the identity and quality of foods (Aguilera 2005).

Extrusion processing is an important technology used for producing a variety of expanded snacks and breakfast cereals having a cellular structure. Microstructure parameters like size and number density of air cells and their contribution to mechanical properties of extrusion-puffed foods have been studied before (Barrett and Peleg 1992; Barrett *et al.* 1994a; Van Hecke *et al.* 1995; Gao and Tan 1996). For example, breaking and plateau stress of cellular extrudates have been correlated to mean cell size (Barrett and Peleg 1992; Barrett *et al.* 1994a), whereas modulus of deformability, Young's modulus and failure strain have been associated with cell size, cell edge thickness and cell density (Van Hecke *et al.* 1995; Gao and Tan 1996).

However, the underlying mechanism relating cellular structure to the mechanics of extruded brittle foams is still not well understood. The limitations of traditional imaging techniques like scanning electron microscopy (SEM) and optical microscopy, which are two dimensional (2-D) and destructive in nature and also provide poor contrast, make it difficult to characterize cellular structure accurately. In fact, most studies on extrusion-puffed foods either ignore their cellular structure or merely present a few cross-sectional images and discuss microstructure qualitatively without making measurements of important features such as cell size distribution or average cell wall thickness (Lai *et al.* 1985; Lee *et al.* 1999; Autio and Salmenkallio-Martilla 2001; Gropper *et al.* 2002).

X-ray microtomography (XMT) is an important development in imaging technology that has eliminated some of the drawbacks of traditional imaging and enabled noninvasive characterization of foam microstructure in three dimensions (Flannery *et al.*1987; Sasov and Van Dyck 1998). XMT-generated images are more conducive to digital image processing than SEM or light microscope images because of "razor-thin" depth of focus and sharp contrast between solid and void areas. XMT has only lately been applied to food foams and has led to some important advances in the understanding of their cellular structure (Whitworth and Alava 1999; Maire *et al.* 2003; Falcone *et al.* 2004, 2005; Lim and Barigou 2004; Trater *et al.* 2005; Babin *et al.* 2006). Our laboratory is one of the first to use XMT for characterizing the cellular structure of extrusion-puffed brittle foams (Trater *et al.* 2005). In our study involving cornstarch-based extrudates, XMT proved to be successful in accurately characterizing several microstructural features that could not be evaluated using traditional imaging techniques such as SEM or optical microscopy. These features included the true cell distribution (bimodal), average diameter (0.58–2.27 mm), cell wall thickness (0.09–0.15 mm) and true void fraction (0.63–0.84). The open wall area fraction (ratio of broken or interconnected wall area to total cell wall area) was measured to be 0.068–0.099, indicating that the extruded brittle foams were primarily closed cellular in nature.

Greater accuracy and objectivity in microstructure measurements have lead to the possibility of applying theoretical models to understand the mechanics of solid foams and eventually to relate sensory properties of crisp or crunchy foods to their cellular structure. One such model was described by Gibson and Ashby (1997) for brittle foams using cubic cell geometry and cellular parameters such as edge length (l) and wall thickness (t_{wall}). To simplify the application of this model, the ratio t_{wall}/l is related to relative density ρ/ρ_s (the ratio of foam density ρ to solid density ρ_s), which is the most important but easy-to-measure "macro" characteristic of solid foams. For true solid foams, $\rho/\rho_s < 0.3$, while values above 0.3 indicate solids containing isolated pores. For closed-cell foams with $\rho/\rho_s < 0.2$, such as starch-based brittle extrudates, the Gibson–Ashby model demonstrates that ρ/ρ_s always scales as t_{wall}/l, with a constant of proportionality near unity. However, in many closed-cell foams, solids are drawn preferentially from the walls to the edges because of a phenomenon called drainage, and a drainage factor ϕ (volume fraction of the solid material present in the cell edges) is used as a correction. This leads to the following more complex relationship that holds true for most closed-cell foams:

$$\frac{t_{\text{wall}}}{l} = 1.4(1-\phi)\frac{\rho}{\rho_s} \tag{1}$$

The Gibson–Ashby model divided a typical stress–strain (or force–deformation) curve for brittle foams under compression into three distinct regions – linear elastic compression, jagged crushing plateau and densification. Each of these regions was described in terms of a characteristic mechanical property, which was a function of mechanical strength of the solid material and cellular parameters.

The linear elastic region during crushing is characterized by the compression modulus (E), which is given by the following equation applicable to closed-cell brittle foams:

$$\frac{E}{E_s} \approx \phi^2\left(\frac{\rho}{\rho_s}\right)^2 + (1-\phi)\frac{\rho}{\rho_s} + \frac{p_0(1-2\nu)}{E_s\left(1-\frac{\rho}{\rho_s}\right)} \tag{2}$$

where E_s is the solid compression modulus; p_0 is the atmospheric pressure (0.1 MPa), and ν is the Poisson's ratio. The ratio E/E_s is also called the relative modulus of the foam. Poisson's ratio ν is mainly based on cell geometry and is estimated to be 0.33 based on data for foams with a wide range of densities.

The crushing plateau for closed-cell brittle foams is characterized by the crushing stress (σ_{cr}), which is described by Eq. (3):

$$\frac{\sigma_{cr}}{\sigma_{fs}} \approx 0.2\left(\phi\frac{\rho}{\rho_s}\right)^{3/2} + (1-\phi)\left(\frac{\rho}{\rho_s}\right) \tag{3}$$

where σ_{fs} is the modulus of rupture of solid material. The ratio σ/σ_{fs} is also called the relative crushing stress of the foam.

The first term in Eqs. (2) and (3) represents the contribution of cell edge bending when there is significant drainage of material from the cell walls to the edges (nontrivial ϕ). This term is derived from the standard theory for bending and failure of beams. The second term in Eqs. (2) and (3) represents the contribution of stresses as a result of cell wall stretching. The third term in Eq. (1) represents the contribution caused by the compression of air inside the cells and is relatively small. The Gibson–Ashby model has been developed and validated primarily for nonfood foams, but its various forms have also been applied to understand the compression behavior of extrusion-puffed cellular foods (Hutchinson *et al.* 1987; Hayter and Smith 1988; Warburton *et al.* 1992) albeit with only limited success.

The Gibson–Ashby model, however, does not describe the "jaggedness" of the crushing plateau of brittle foods, which has also been associated with the sensory properties of crispness and crunchiness (Barrett *et al.* 1994b; Barrett

and Peleg 1995). Previous studies have used fractal analysis to quantify the jaggedness of the force–deformation curves during compression of expanded extrudates (Barrett *et al.* 1992; Barrett *et al.* 1994b; Barrett and Peleg 1995). Fractal analysis involves complex mathematical treatments like fast Fourier transform and is not easy to relate to microstructure parameters. Bouvier *et al.* (1997) extracted several parameters from the force–deformation curve during puncture testing of expanded extrudates. These parameters included the number of structural ruptures, average specific force of structural ruptures, average puncture force and crispness work. This is a simpler method to quantify the jagged mechanical response of brittle foams, but the study provides only limited understanding of how jaggedness is affected by cellular structure.

The primary objective of this study was to test the validity of the Gibson–Ashby model for describing mechanical properties of cellular extrudates and to relate microstructure features of these brittle foams to their mechanical response including jaggedness of the force–deformation curve. Utilization of the noninvasive XMT technique for accurate characterization of cellular structure would provide greater meaning to this endeavor, as compared with previous studies. This study hopes to be an initial step toward developing models that would help in the design of crisp and crunchy food products with targeted mechanical properties and sensory attributes.

MATERIALS AND METHODS

Extrusion Processing

Unmodified cornstarch (~25% amylose and 75% amylopectin, Cargill Gel 03457, Cargill, Inc., Minneapolis, MN) was used as the only ingredient for all extrusion runs. A Wenger TX-52 twin-screw extruder (Wenger Manufacturing, Inc., Sabetha, KS), with screw diameters of 52 mm, L/D ratio of 16:1, medium-shear screw profile (Fig. 1) and circular die opening of 3.3 mm, was used to process all materials. Cornstarch was extruded at four in-barrel moisture contents (23, 25, 27 and 29%, wet basis [wb]) and three screw speeds (200, 300 and 400 rpm). The feed rate of raw material was 60 kg/h. Water flow to the preconditioner was maintained at a constant 9 kg/h. Water flow in the extruder was adjusted to 0, 2, 4 or 6 kg/h, depending on treatment. Extruder conditions were allowed to stabilize for approximately 10 min before samples were collected. The product was cut, immediately after exiting the extruder die, with a face-mounted rotary cutter turning at 690 rpm, and was dried at 100C with a double-pass dryer/cooler (4800 Series, Wenger Manufacturing, Inc.) adjusted for 15-min retention time (7.5 min each for the top and bottom

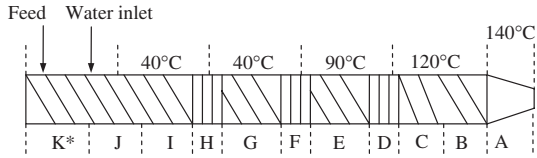

Section	Number of elements	Element length, mm	Element description
A	1	78	¾ pitch, double flighted, conical
B	1	78	¾ pitch, double flighted
C	1	52	½ pitch, double flighted
D	1	26	kneading block, forward
E	1	78	¾ pitch, double flighted
F	1	26	kneading block, forward
G	1	78	¾ pitch, double flighted
H	1	26	kneading block, forward
I	1	78	¾ pitch, double flighted
J	2	78	full pitch, double flighted
K	2	78	¾ pitch, double flighted

FIG. 1. DIAGRAM OF THE EXTRUDER SCREW CONFIGURATION, WATER INJECTION SITES AND BARREL TEMPERATURES USED FOR ALL TREATMENTS
Lengths of screw elements are not to scale. The asterisk (*) indicates that the first two elements of the right shaft at the inlet (K) are $^{3}/_{4}$ pitch, single flighted.

belts). Cooling was accomplished at 24C, with a 5-min retention time on the cooling belt.

Image Acquisition and Processing for Determining Microstructure Parameters

Representative samples from two replicate extrusion runs were selected for image analysis. A desktop XMT imaging system (model 1072, 20–100 kV/0–250 μA, SkyScan, Aartselaar, Belgium) set at 40 kV/100 μA (to obtain optimum contrast between solid and gaseous phases) was used to scan the samples. For each sample, a set of 15 2-D virtual "slices" was obtained after reconstruction. Calculations of three-dimensional (3-D) microstructural parameters were based on measurement of 2-D features from each slice using image analysis software (Scion Image for Windows, Scion Corp., Frederick, MD), and their subsequent integration over all the slices. These 2-D features included individual cell perimeters and void areas, and overall solid and void areas for each slice. The computed 3-D parameters included volume weighted average cell diameter ($\overline{D}$), cell wall thickness (t_{wall}) and cell number density (N). Details of XMT scanning, image reconstruction, thresholding, measurement of 2-D features and computation of 3-D microstructural parameters have been described previously (Trater *et al.* 2005).

Analysis of Mechanical Properties

Thirty samples with approximately the same dimensions (diameter and height) were chosen from each treatment. Force–deformation data for each extrudate were obtained using a texture analyzer (TA-XT2, Stable Micro Systems, Godalming, U.K.) in the compression mode. A test probe of 38-mm diameter was used at a speed of 10 mm/s to compress samples to 90% of their original height. A stress–strain curve was determined from the force deformation data and sample dimensions. *C*ompression modulus was calculated as the slope of the linear viscoelastic region before first rupture (or fracture). Crushing stress was calculated as the mean stress from the point of first rupture (or fracture) to first point of densification.

For determining jaggedness parameters, a Kramer shear press consisting of five 1.5-mm thick plates was used in conjunction with the texture analyzer. Five samples were used at a time for each test, and three replicates per treatment were conducted. The test speed was 8 mm/s in the compression mode. A force–deformation curve was obtained, and the number of peaks, n, integral of the curve, S (or area below the curve from 0 to 100% strain), and distance of compression, d, were computed. From n, S and d values, the following parameters were calculated (Bouvier *et al.* 1997):

$$N_{sr} = \frac{n}{d}\left(\text{mm}^{-1}\right) \tag{4}$$

$$F_{cr} = \frac{S}{d}(\text{N}) \tag{5}$$

$$W_c = \frac{F_c}{N_{sr}} = \frac{S/d}{n/d}(\text{N}\cdot\text{mm}) \tag{6}$$

where N_{sr} is the number of spatial ruptures; F_{cr} is the average crushing force, and W_c is crispness work.

Physical Properties (Piece and Solid Densities)

Piece densities (ρ) were obtained by the rapeseed displacement method. Solid densities (ρ_s) were obtained for the ground extrudate by using a helium pycnometer (model NVP-1, Quantachrome, Boynton Beach, FL). All density measurements were adjusted to 0% moisture basis to eliminate the contribution of water to material density. Relative density (ρ/ρ_s) was computed from piece and solid densities.

Experimental Design and Statistical Analysis

A 3×4 factorial design, with four levels of in-barrel moisture and three levels of screw speed, was used to produce extrudates with different microstructures. Each extrusion treatment was replicated twice. For measurement of mechanical properties of extrudates, 30 replicates were conducted for the compression test, and three for the Kramer shear test. Microstructural parameters were measured using one representative sample from each replicate treatment. Nonlinear regression using the least square method was used for fitting data to model equations, and corresponding R^2 values were generated to test the goodness of fit. The "Pearson" function of Excel software (2002 edition, Microsoft Corp., Redmond, WA) was used for finding the Pearson's coefficient of correlation (r) between any two data sets. To provide descriptive terms to the degree of correlation, criteria outlined by Franzblau (1958) were used ($|r| < 0.20$, negligible; $|r| = 0.20$–0.40, low; $|r| = 0.40$–0.60, moderate; $|r| = 0.60$–0.80, marked; and $|r| > 0.80$, high).

RESULTS AND DISCUSSION

Microstructure of Cornstarch Extrudates

Representative 2-D XMT slices of samples from each treatment are shown in Fig. 2. Extrudates exhibited different cell structures depending on the in-barrel moisture and screw speed, but were mostly closed cell in nature as has been observed by our research group previously (Trater *et al.* 2005). The cell diameter($\bar{D}$), cell wall thickness (t_{wall}) and cell number density (N) ranged from 2.07 to 6.32 mm, 0.13–0.25 mm and 18–146 cells/cm^3, respectively. Cell diameter increased, and cell number density decreased with decreasing in-barrel moisture or increasing screw speed. No specific trend was observed for cell wall thickness at different in-barrel moistures and screw speeds. Average solid density for all samples was 1,350 kg/m^3. Piece density (ρ) ranged from 128 to 302 kg/m^3. The piece density decreased, indicating greater expansion, with decreasing in-barrel moisture or increasing screw speed. The main driving force for expansion of extrudates is the mechanical energy input. Reduced in-barrel moisture would lead to an increase in melt viscosity, which in turn would increase the mechanical energy input and therefore increase expansion. Increase in extruder screw speed would also lead to higher mechanical energy input, and therefore increased expansion. Detailed analyses of the effect of process parameters on the microstructural characteristics of these extrudates will be presented in a separate article. However, increase in cell diameter and decrease in cell number density with higher overall

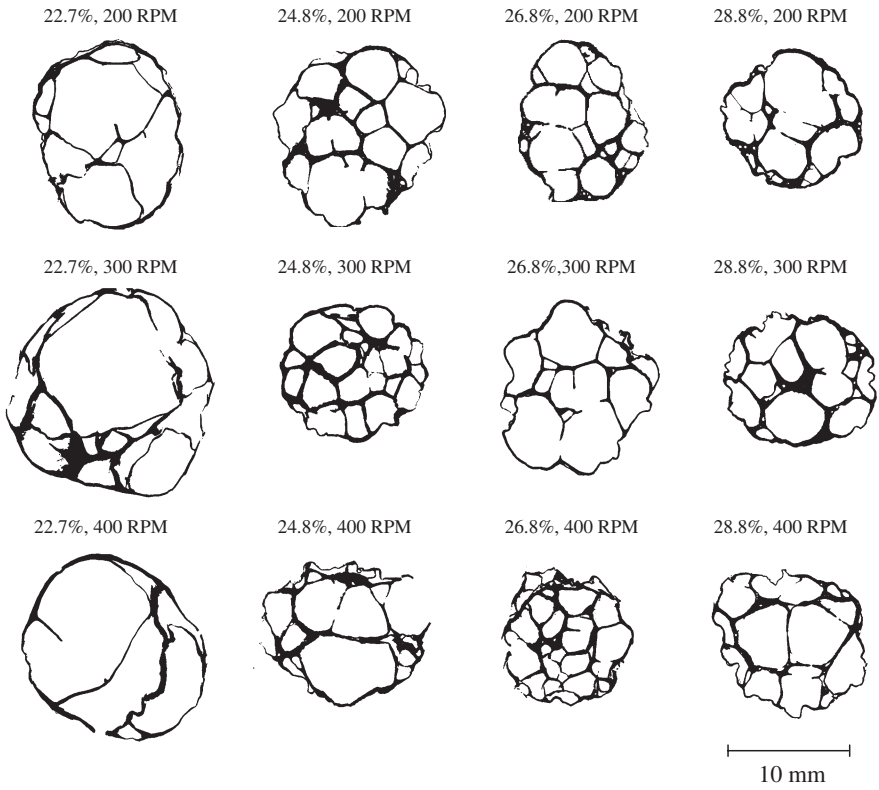

FIG. 2. X-RAY MICROTOMOGRAPHY IMAGES OF REPRESENTATIVE TWO-DIMENSIONAL SLICES (PERPENDICULAR TO THE DIRECTION OF EXTRUSION) OF FOAMS FROM EACH TREATMENT
All images correspond to the scale indicated on the bottom right.

expansion of extrudates is consistent with previously observed results (Trater *et al.* 2005), and has been attributed to the phenomena of cell expansion and coalescence occurring simultaneously.

Relationship Between Macro- and Microstructural Parameters

Figure 3A shows a plot of relative density (ρ/ρ_s) versus cell wall thickness to cell diameter ratio ($t_{wall}/\overline{D}$). For the most part, $\rho/\rho_s < 0.2$, an important condition for applicability of the Gibson–Ashby model equations described earlier. There was also a marked degree of correlation ($r = 0.72$) between ρ/ρ_s and $t_{wall}/\overline{D}$, indicating the validity of Eq. (1). The ρ/ρ_s and $t_{wall}/\overline{D}$ data were

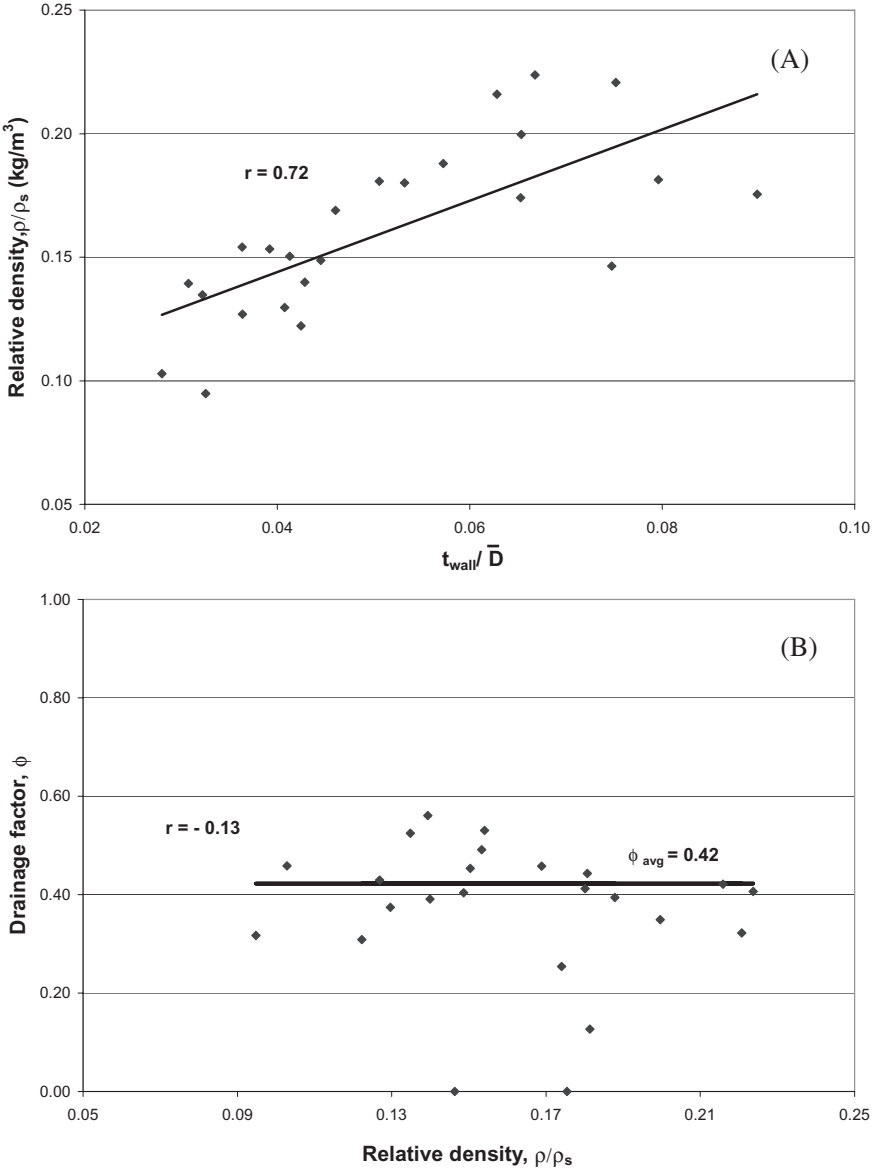

FIG. 3. (A) RELATIVE DENSITY (ρ/ρ_s) VERSUS CELL WALL THICKNESS TO CELL DIAMETER RATIO ($t_{wall}/\bar{D}$) AND (B) DRAINAGE FACTOR (ϕ) VERSUS RELATIVE DENSITY Solid line in (A) represents the linear trend line for the data set. Horizontal solid line in (B) represents average value of ϕ (= 0.42) after excluding some outliers.

fitted to Eq. (1) to obtain the drainage factor (ϕ) for each treatment. The average cell diameter ($\bar{D}$) is different from the edge length (l), so a scaling factor, $l = 0.36\bar{D}$, was used based on relationships for typical closed-cell foams (Gibson and Ashby 1997). No particular trend was observed for ϕ versus ρ/ρ_s ($r = -0.13$, Fig. 3B). In fact, ϕ was within a narrow band ranging from 0.31 to 0.56, except for a few outliers (a couple of ϕ values were negative, which did not make sense physically so these were taken as 0). The average value of ϕ within this band was calculated to be 0.42.

Mechanical Profile of Extruded Cornstarch

Typical stress–strain curves of extrudates under compression are shown in Fig. 4. Stress levels rose linearly with strain until the first fracture, followed by a crushing region with multiple peaks. Densification occurred at approximately 85–90% strain. For cornstarch extruded at the lowest in-barrel moisture (22.7%), as compression of the sample continued, a fracture point was reached and the sample broke into two pieces. Compression of the remaining pieces resumed shortly thereafter, creating a brittle crushing plateau with numerous peaks. For extrudates processed at 24.8, 26.8 and 28.8% in-barrel moisture, the sample collapsed and broke into numerous pieces after fracturing. For these treatments, peaks in the crushing region were relatively higher and so was the drop-off force after each fracture, as compared with treatments with 22.7% in-barrel moisture. As detailed previously in this article, *c*ompression modulus and crushing stress were calculated from the stress–strain curves, while the jaggedness parameters were extracted from the force–deformation curves obtained from the Kramer shear test.

Microstructure–Mechanical Property Relationships

Figure 5 shows plots of extrudate compression modulus (E) and crushing stress (σ_{cr}) versus $\bar{D}$. Compression modulus ranged between 2.2 and 7.8 MPa, and crushing stress between 42 and 240 kPa. High correlations were observed ($r = -0.81$) between both mechanical properties and $\bar{D}$. It was clear that both E and σ_c decreased with an increase in cell diameter, which indicated a general weakening of the foam structure with greater expansion of the cells. Some previous studies have observed similar relationships between mechanical properties of expanded extrudates and their average cell diameter (Barrett and Peleg 1992; Barrett *et al.* 1994a; Van Hecke *et al.* 1995). Compression modulus (E) and crushing stress (σ_{cr}) were also plotted versus $t_{wall}/\bar{D}$ (Fig. 6). Moderate to marked correlations were observed for E and σ_{cr} with $t_{wall}/\bar{D}$ ($r = 0.64$ and 0.54, respectively). This demonstrated the combined effect of cell diameter and cell wall thickness on the mechanical properties of the starch-based brittle foams. According to standard beam theory, from which the

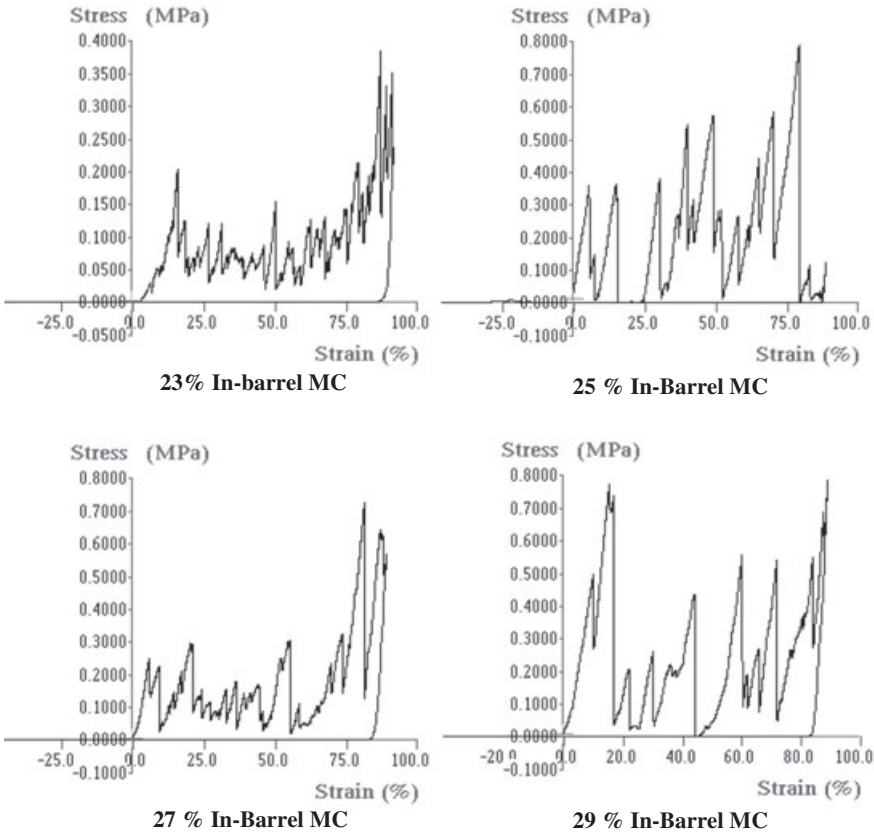

FIG. 4. REPRESENTATIVE STRESS–STRAIN CURVES FOR CORNSTARCH-BASED BRITTLE FOAMS EXTRUDED AT 23, 25, 27 AND 29% IN-BARREL MOISTURES AT 200-rpm SCREW SPEED
MC, moisture content.

Gibson–Ashby model is partially derived, increasing thickness and decreasing length of beams lead to higher stiffness and failure strength. It is clear from our data that foams with higher $t_{wall}/\overline{D}$, which means thicker cell walls and smaller cell diameters, had higher compression modulus and crushing stress as compared to foams with lower $t_{wall}/\overline{D}$ (thinner walls and larger cell diameters). Lower correlation coefficients with respect to the ratio $t_{wall}/\overline{D}$, as compared with $\overline{D}$, do not necessarily imply that the compression modulus and crushing stress are more closely related to the latter and that the Gibson–Ashby model is inadequate. Instead, it may indicate that the relationship between the mechanical properties and $t_{wall}/\overline{D}$ is more nonlinear. The latter is definitely true, as can be seen from the Gibson–Ashby model equations (Eqs. 2 and 3).

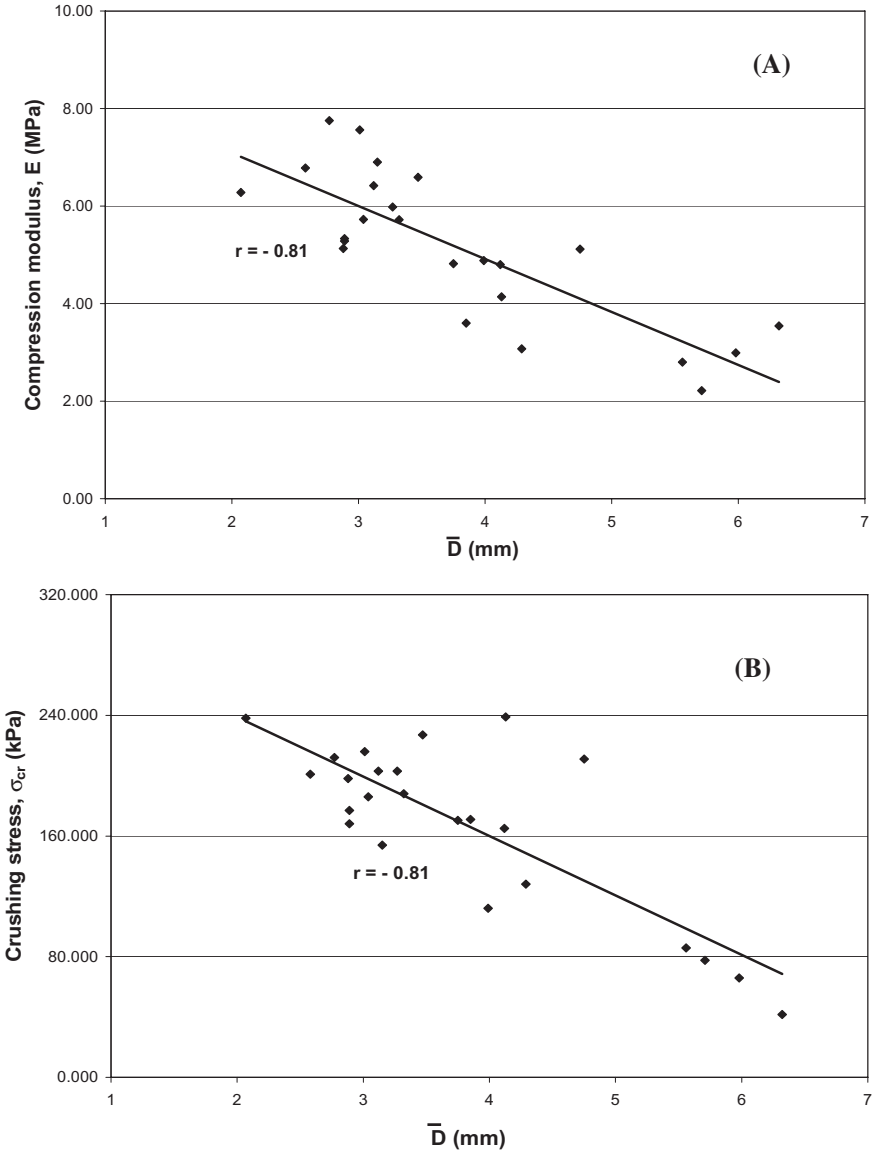

FIG. 5. (A AND B) COMPRESSION MODULUS (E) AND CRUSHING STRESS (σ_{cr}) VERSUS AVERAGE CELL DIAMETER ($\bar{D}$) OF EXTRUDED CORNSTARCH-BASED BRITTLE FOAMS
Solid lines represent linear trend lines for the data sets.

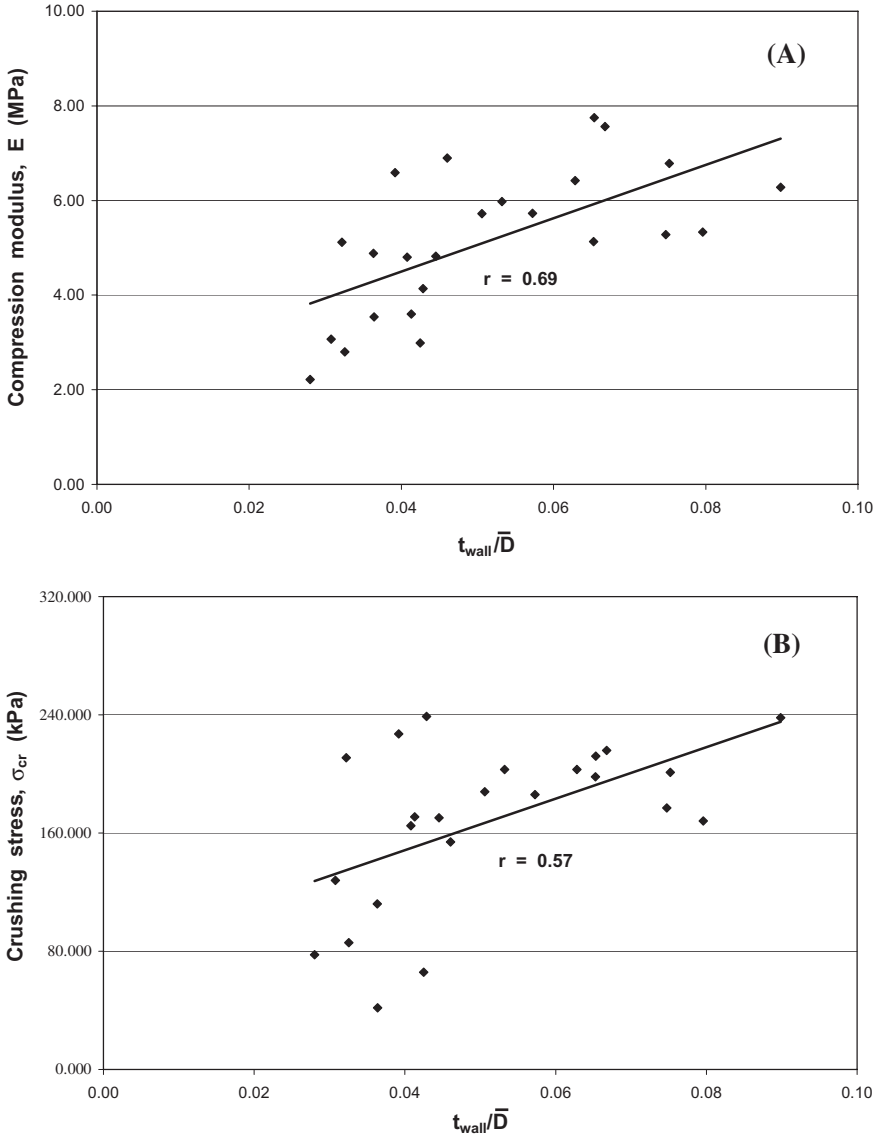

FIG. 6. (A AND B) COMPRESSION MODULUS (E) AND CRUSHING STRESS (σ_{cr}) VERSUS CELL WALL THICKNESS TO CELL DIAMETER RATIO ($t_{wall}/\bar{D}$) OF EXTRUDED CORNSTARCH–BASED BRITTLE FOAMS
Solid lines represent linear trend lines for the data sets.

It was difficult to measure the mechanical properties of the solid matrix with precision as has been observed in previous studies as well (Hutchinson *et al.* 1987; Gibson and Ashby 1997). Moreover, it would be inappropriate to measure these properties for unfoamed material involving very different processing conditions; therefore, E_s (52.64 MPa) and σ_{fs} (1.74 MPa) were obtained by fitting experimental data to Eqs. (2) and (3), respectively. The solid lines in Fig. 7 represent the best fit curves obtained using nonlinear regression (least square method). The average value of ϕ (= 0.42) was used for the fitting. The dotted curves in Fig. 8 represent the predicted mechanical properties of extruded foams using the upper and lower bounds of ϕ (0.56 and 0.31, respectively). The compression modulus data had a much better fit ($R^2 = 0.72$) with the Gibson–Ashby model than the crushing stress data ($R^2 = 0.41$), although about two-thirds of the data points for both E and σ_{cr} lay within the upper and lower bounds. Gibson and Ashby (1997) also observed a relatively poorer fit of σ_{cr} data for brittle glass and metal foams to their model. They attributed this to inaccuracies in estimation of the cell wall modulus of rupture (σ_{fs}).

Figure 8 shows the plot of the jaggedness parameters (F_{cr} and W_c), obtained from the Kramer shear test, versus the microstructure features of the extrudates. The average crushing force ranged between 22 and 67 N, and crispness work between 6.4 and 22 N·mm. Both average crushing force and crispness work had marked to high correlations with cell diameter ($r = -0.79$ and -0.81, respectively). As expected, both F_{cr} and W_c increased with a decrease in cell diameter, indicating that more force and work were needed to deform/fracture smaller-size cells. This was similar to the observation for compression modulus and crushing stress, which showed a high negative correlation with $\bar{D}$. The number of spatial ruptures (N_{sr}) of extrudates ranged between 2.6 and 3.6 mm^{-1} (data not shown). It was expected that the number of spatial ruptures during deformation would increase with higher cell number density. On the contrary, a moderate negative correlation ($r = -0.48$) was observed between N_{sr} and N. This gave a unique insight, not provided by the Gibson–Ashby model, into the mechanics of brittle foam deformation. As foams deform under compression, the resultant stress is transmitted uniformly through the microstructure. Larger cells with walls that are relatively thin and/or weakened as a result of cracks represent "weak spots" in the structure. These weaker cells reach their fracture point earlier. Often, more than one cell fracture at the same time, with each peak in the force–deformation curve representing the combined effect. It is likely that foams with higher N have numerous smaller cells fracturing at the same time, thus resulting in lower N_{sr}. This also explains the higher magnitude of the peaks as compared with foams with lower N.

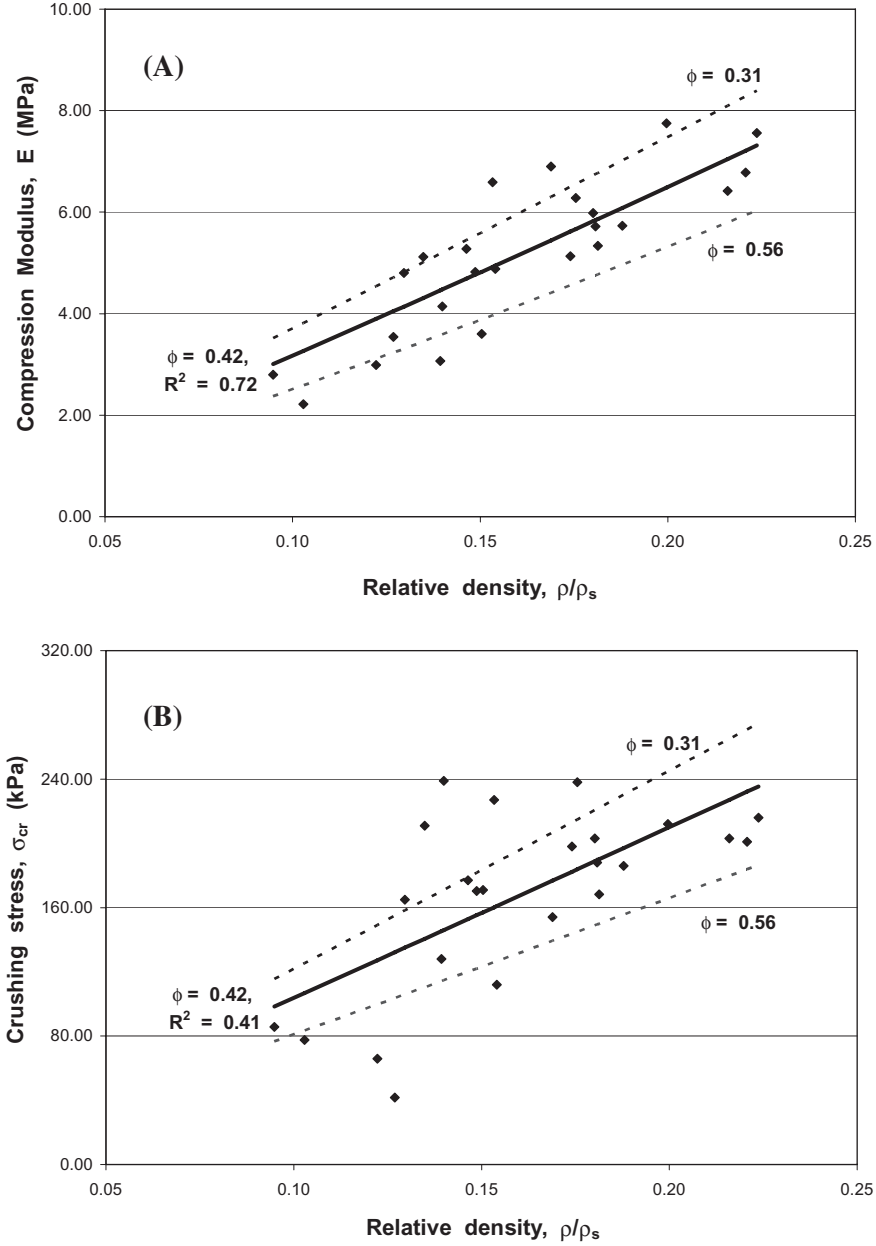

FIG. 7. (A AND B) COMPRESSION MODULUS (E)AND CRUSHING STRESS (σ_{cr}) DATA FITTED TO THE GIBSON–ASHBY MODEL (SOLID LINES) USING THE AVERAGE VALUE OF DRAINAGE FACTOR (ϕ) ($\phi = 0.42$)
The dotted lines represent predicted mechanical properties using the upper and lower bounds of ϕ (0.56 and 0.31, respectively).

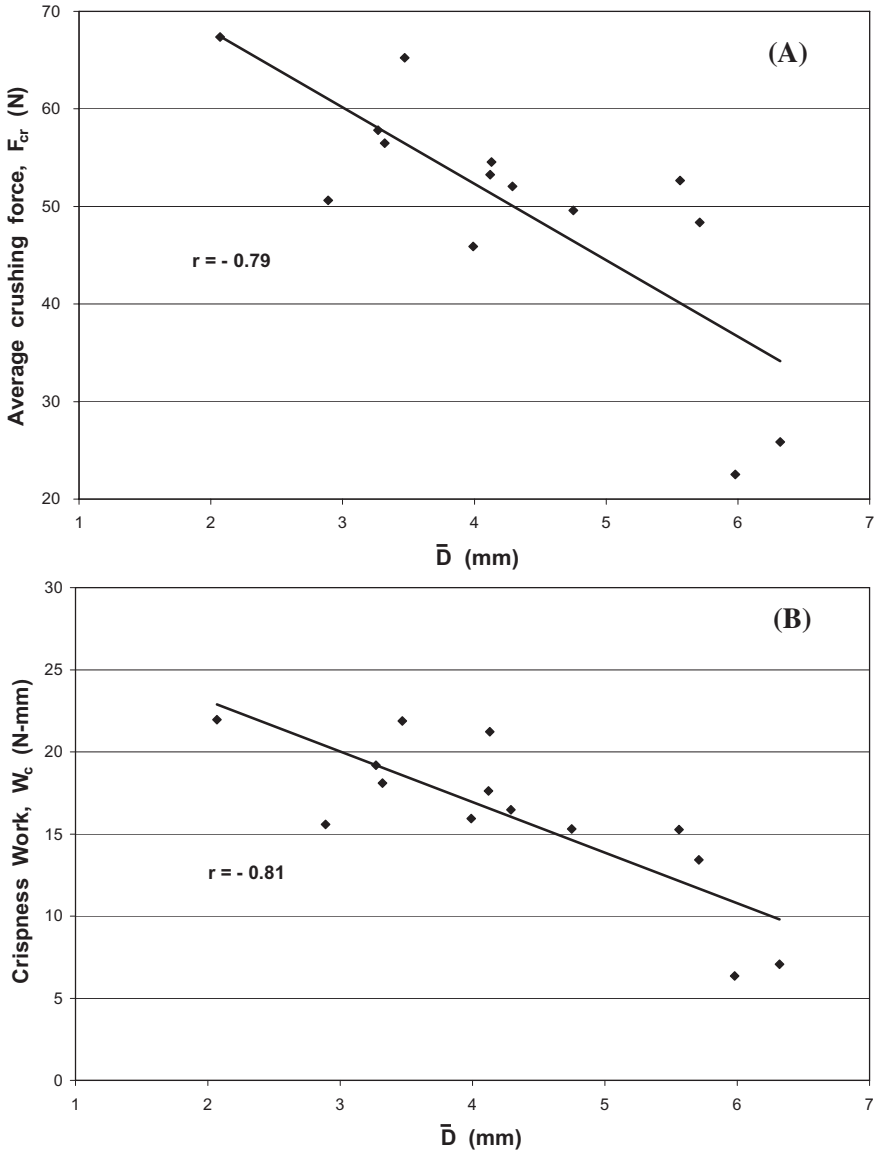

FIG. 8. (A AND B) JAGGEDNESS PARAMETERS, AVERAGE CRUSHING FORCE (F_{cr}) AND CRISPNESS WORK (W_c), VERSUS AVERAGE CELL DIAMETER ($\bar{D}$) OF EXTRUDED CORNSTARCH-BASED BRITTLE FOAMS
Solid lines represent linear trend lines for the data sets.

Shortcomings of the Gibson–Ashby Model

As described earlier, the compressive modulus data for brittle foams had a reasonably good fit ($R^2 = 0.72$) with the Gibson–Ashby model; however, crushing stress data did not fit as well ($R^2 = 0.41$). The Gibson–Ashby equations were derived using some simplifying assumptions including cubic cell geometry and a uniform microstructure. In reality, cell shapes are more complex, and microstructure features, such as cell diameter and wall thickness, are nonuniform and distributed over a range (Fig 2). Moreover, the constants associated with various terms in the model equations are either estimations or fitted using available data. The Gibson–Ashby equations are also inadequate for modeling the jaggedness of the force–deformation curve. Other models that can overcome some of the previously mentioned shortcomings should be explored. One such model has been described by Cuitino and Zheng (2003) based on a thin-walled spherical unit cell. This micromechanical model takes into account cell size distribution of the foam (average radius, variance and skewness) and the mechanics of cell wall bending and stretching. It uses a strain energy density function and averages the response of unit cells of different sizes using Taylor averaging. Cuitino and Zheng (2003) have successfully used this approach to model the deformation behavior of yellow cake. Further details of this model is beyond the scope of the current study; however, there is potential of applying it to estimate the jagged response curve associated with deformation of brittle foams.

CONCLUSIONS

XMT was used to characterize the 3-D microstructure features of extruded starch-based brittle foams. The compressive modulus and crushing stress of the foams were measured, and the jaggedness parameters (number of spatial ruptures, average crushing force and crispness work) were also extracted from force–deformation curves. Microstructure data, such as average cell diameter, cell wall thickness and drainage factor, were utilized to assess the applicability of the Gibson–Ashby model toward the prediction of mechanical properties of brittle foams. Compression modulus data showed a good fit to the Gibson–Ashby model, whereas crushing stress data had a relatively poor fit. Moderate to high correlations were observed between all mechanical properties and microstructure features. This study furthered understanding of the deformation mechanism of brittle foams and is an important step toward the ability to better design crisp and crunchy food products with desired textures. However, assumptions such as cubic cell geometry and uniform microstructure limit the applicability of the Gibson–Ashby model.

Other models, which can overcome these shortcomings as well as predict the jagged deformation response of brittle foams, should also be evaluated in the future. Noninvasive imaging techniques such as XMT will be crucial in this endeavor as it enables a degree of cellular characterization that is much higher than possible by SEM or optical microscopy.

ACKNOWLEDGMENTS

This study was funded by the National Research Initiative (NRI) Competitive Grants Program (Award Number 2003-35503-13999) of the USDA Cooperative State Research, Education, and Extension Service. The authors would like to thank Mr. Eric Maichel for his technical assistance, and Wenger Manufacturing, Inc. and Micro Photonics, Inc. (Allentown, PA) for their continued support to the extrusion laboratory at Kansas State University. This is Contribution Number 06-257-5 from the Kansas Agricultural Experiment Station, Manhattan, KS.

REFERENCES

AGUILERA, J.M. 2005. Why food microstructure? J. Food Eng. *67*, 3–11.

AUTIO, K. and SALMENKALLIO-MARTILLA, M. 2001. Light microscopic investigations of cereal grains, doughs and breads. Lebensm.-Wiss. Technol. *34*, 18–22.

BABIN, P., DELLA VALLE, G., CHIRON, H., CLOETENS, P., HOSZOWSKA, J., PERNOT, P., REGUERRE, A.L., SALVO, L. and DENDIEVEL, R. 2006. Fast X-ray tomography analysis of bubble growth and foam setting during breadmaking. J. Cereal Sci. *43*, 393–397.

BARRETT, A.H. and PELEG, M. 1992. Extrudate cell structure-texture relationships. J. Food Sci. *57*(5), 1253–1257.

BARRETT, A.H. and PELEG, M. 1995. Applications of fractal analysis to food structure. Lebensm.-Wiss. Technol. *28*, 553–563.

BARRETT, A.M., NORMAND, M.D., PELEG, M. and ROSS, E. 1992. Characterization of the jagged stress-strain relationships of puffed extrudates using the fast Fourier transform and fractal analysis. J. Food Sci. *57*(1), 227–235.

BARRETT, A.H., CARDELLO, A.V., LESHER, L.L. and TAUB, I.A. 1994a. Cellularity, mechanical failure and texture perception of corn meal extrudates. J. Texture Studies *25*, 77–95.

BARRETT, A.H., ROSENBERG, S. and ROSS, E.W. 1994b. Fracture intensity distributions during compression of puffed corn meal extrudates: Method of quantifying fracturability. J. Food Sci. *59*(3), 617–620.

BOUVIER, J.M., BONNEVILLE, R. and GOULLIEUX, A. 1997. Instrumental methods for the measurement of extrudate crispness. Agro-Food-Industry Hi-Tech. *8*(1), 16–19.

CUITINO, A.M. and ZHENG, S. 2003. Taylor averaging on heterogeneous foams. J. Compos. Mater. *37*(8), 701–713.

FALCONE, P.M., BAIANO, A., ZANINI, F., MANCINI, L., TROMBA, G., MONTANARI, F. and DEL NOBILE, M.A. 2004. A novel approach to the study of bread porous structure: Phase-contrast X-ray microtomography. J. Food Sci. *69*(1), 38–43.

FALCONE, P.M., BAIANO, A., ZANINI, F., MANCINI, L., TROMBA, G., DREOSSI, D., MONTANARI, F., SCUOR, N. and DEL NOBILE, M.A. 2005. Three-dimensional quantitative analysis of bread crumbs by X-ray microtomography. J. Food Sci. *70*(4), 265–272.

FLANNERY, B.P., DECKMAN, H.W., ROBERGE, W.G. and D'AMICO, K.L. 1987. Three-dimensional x-ray microtomography. Science *237*, 1439–1444.

FRANZBLAU, A. 1958. *A Primer of Statistics for Non-Statistician*, Harcourt Brace and World, New York, NY.

GAO, X. and TAN, J. 1996. Analysis of expanded-food texture by image processing. Part II. Mechanical properties. J. Food Process Eng. *19*, 445–456.

GIBSON, L.G. and ASHBY, M.F. 1997. *Cellular Solids: Structure and Properties*, Cambridge University Press, Cambridge, U.K.

GROPPER, M., MORARU, C. and KOKINI, J.L. 2002. Effect of specific mechanical energy on properties of extruded protein-starch mixtures. Cereal Chem. *79*, 429–433.

HAYTER, A.L. and SMITH, A.C. 1988. The mechanical properties of extruded food foams. J. Mater. Sci. *23*, 736–743.

HUTCHINSON, R.J., SIODLAK, G.D.E. and SMITH, A.C. 1987. Influence of processing variables on the mechanical properties of extruded maize. J. Mater. Sci. *22*, 3956–3962.

LAI, C.S., DAVIS, A.B. and HOSENEY, R.C. 1985. The effect of a yeast protein concentrate and some of its components on starch extrusion. Cereal Chem. *62*(4), 293–300.

LEE, E.Y., RYU, G.H. and LIM, S.-T. 1999. Effects of processing parameters on physical properties of corn starch extrudates expanded using supercritical CO_2 injection. Cereal Chem. *76*(1), 63–69.

LIM, K.S. and BARIGOU, M. 2004. X-ray micro-computed tomography of cellular food products. Food Res. Int. *37*, 1001–1012.

MAIRE, E., FAZEKAS, A., SALVO, L., DENDIEVEL, R., YOUSSEF, S., CLOENTENS, P. and LETANG, J.M. 2003. X-ray tomography applied to

the characterization of cellular materials. Related finite element modeling problems. Compos. Sci. Technol. *63*, 2431–2443.

SASOV, A. and VAN DYCK, D. 1998. Desktop X-ray microscopy and microtomography. J. Microsc. *191*(2), 151–158.

TRATER, A.M., ALAVI, S. and RIZVI, S.S.H. 2005. Use of non-invasive X-ray microtomography for characterizing microstructure of extruded biopolymer foams. Food Res. Int. *38*, 709–719.

VAN HECKE, E., ALLAF, K. and BOUVIER, J.M. 1995. Texture and structure of crispy-puffed food products. I: Mechanical properties in bending. J. Texture Studies *26*, 11–25.

WARBURTON, S.C., DONALD, A.M. and SMITH, A.C. 1992. Structure and mechanical properties of brittle starch foams. J. Mater. Sci. *27*, 1469–1474.

WHITWORTH, M.B. and ALAVA, J.M. 1999. The imaging and measurement of bubbles in bread doughs. In *Bubbles in Food* (G.M. Campbell, C. Webb, S.S. Pandiella and K. Niranjan, eds.) pp. 221–231, Eagan Press, St. Paul, MN.